

Thermoelectric Energy Conversion with Solid Electrolytes

Terry Cole

Direct conversion of heat energy to electrical energy—that is, conversion without the use of moving mechanical parts—has both aesthetic and practical appeal. Several devices (1) for thermoelectric direct conversion have been developed. The Seebeck effect, thermionic, and magnetohydrodynamic generators are familiar examples. None of these

with the well-known heat engines in which a working fluid is carried around a thermodynamic cycle. They are Carnot-limited in efficiency. Many types of TRES were investigated in the 1950's and 1960's in the search for improved methods of converting the thermal output of nuclear reactors to electrical power.

Summary. The alkali metal thermoelectric converter (AMTEC) is a device for the direct conversion of heat to electrical energy. The sodium ion conductor beta"-alumina is used to form a high-temperature regenerative concentration cell for elemental sodium. An AMTEC of mature design should have an efficiency of 20 to 40 percent, a power density of 0.5 kilowatt per kilogram or more, no moving parts, low maintenance requirements, high durability, and efficiency independent of size. It should be usable with high-temperature combustion, nuclear, or solar heat sources. Experiments have demonstrated the feasibility of the AMTEC and confirmed the theoretical analysis of the device. A wide range of applications from aerospace power to utility power plants appears possible.

direct converters has been widely adopted because of practical problems such as parasitic heat loss or lack of a critical material with the physical properties necessary for high efficiency and good durability.

Among the less well known direct thermoelectric converters are the thermally regenerative electrochemical systems (TRES). These devices are closed electrochemical systems which include electrochemical cells that produce electrical power. The reactants for these cells are regenerated within the device by thermal energy from a heat source which flows through the device to a heat sink. TRES have also been called electrochemical heat engines, by analogy

All of the early TRES were plagued by practical problems such as inefficient heat exchange, electrode polarization, slow chemical regeneration kinetics, materials separation problems, and corrosion. Power densities of these early systems were usually limited to a few tens of milliwatts per square centimeter of electrode area, and thermoelectric efficiencies were below 5 percent. A comprehensive review of TRES has been prepared by Chum and Osteryoung (2). The development of beta-alumina solid electrolytes has made possible a new TRES, the alkali metal thermoelectric converter, which is capable of high power and high efficiency and avoids the practical difficulties of the earlier systems.

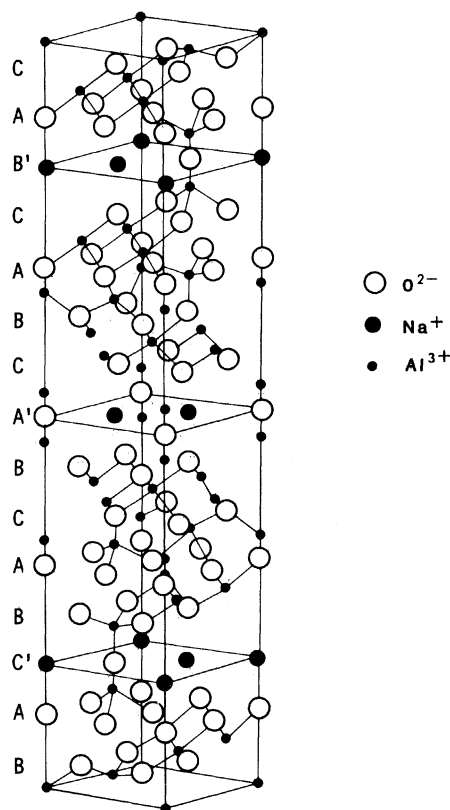
Background

In 1962, during early stages of work on the sodium-sulfur battery, J. T. Kummer at the Ford Motor Company Scientific Laboratory conceived the thermally powered sodium concentration cell, based on the unique electrical properties of beta-alumina solid electrolyte. Kummer and his colleague N. Weber experimentally demonstrated the feasibility of such a device and obtained a patent on it in 1968 (3). Shortly after issuance of the patent, Weber began research on the new thermoelectric converter in collaboration with T. Cole and T. K. Hunt. This new device has come to be called the sodium heat engine (SHE) or, somewhat more descriptively, the alkali metal thermoelectric converter (AMTEC). It is the first TRES with efficiency and power density high enough to be competitive with conventional heat engines. Several reports describing work on the AMTEC or SHE have appeared (4-9). The device is currently being investigated by groups at the Ford Motor Company, Jet Propulsion Laboratory, and General Electric Company.

The critical material in the operation of the AMTEC is beta"-alumina, a member of the class of materials known as solid electrolytes or fast ion conductors (10, 11). These materials have ionic conductivities much larger than their electronic conductivities and thus can act as permselective barriers in electrochemical devices. Beta"-alumina solid electrolyte (BASE) is a transparent crystalline solid melting at 2253 K, has the nominal composition $\text{Na}_{5/3}\text{Li}_{1/3}\text{Al}_{32/3}\text{O}_{17}$, and is usually fabricated as a dense microcrystalline sintered ceramic. It is inert to reaction with elemental sodium at temperatures as high as 1300 K. Its Na^+ conductivity at 1000 K is $0.7 \text{ ohm}^{-1} \text{ cm}^{-1}$.

The unique electrical properties of BASE arise from its crystal structure, which consists of extended layers of aluminum oxide separated by layers con-

Terry Cole is chief technologist at the Jet Propulsion Laboratory and a senior research associate in the Division of Chemistry and Chemical Engineering, California Institute of Technology, Pasadena 91125.



taining only sodium and oxygen ions. Figure 1 shows a view of the unit cell structure of beta''-alumina. The symmetry and spacing of the close-packed O²⁻ ions above and below the Na⁺ planes produce a low activation energy barrier for jumping of Na⁺ from one site to the next, with the result that there is rapid diffusional motion of sodium ions in these planes. Sintered polycrystalline BASE in shapes such as tubes and plates is available commercially (12).

Principles of Operation

The operating cycle of the AMTEC is illustrated diagrammatically in Fig. 2. A closed vessel is divided into two regions by a separator of BASE and a pump. Liquid sodium fills the upper region, which is maintained at a temperature T_2 in the range 900 to 1300 K by an external heat source. In this temperature range the vapor pressure of sodium is 0.05 to 2.5 atm (5.0×10^3 to 2.5×10^5 Pa). The lower region, containing mostly sodium vapor and a small amount of liquid sodium, is in contact with a heat sink at T_1 in the range 400 to 800 K, which produces a sodium vapor pressure range of 10^{-9} to 10^{-2} atm (10^{-4} to 10^3 Pa). A porous electrode covers the low-pressure side of the BASE separator. Electrical leads making contact with the porous elec-

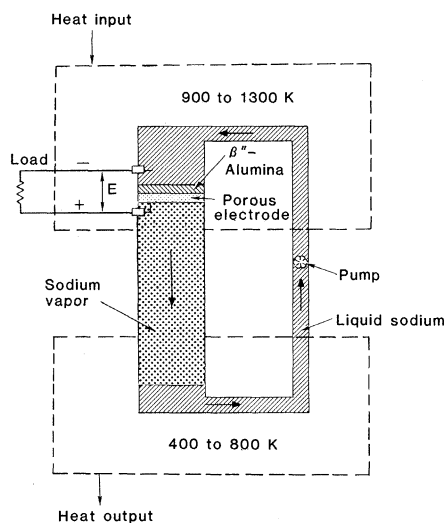
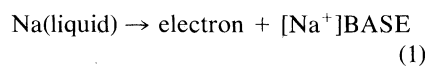


Fig. 1 (left). Unit cell of beta''-alumina (10). The stabilizing ions for this structure such as Li⁺ and Mg²⁺, which reside in the aluminum-oxygen spinel layers, are not shown here. The planes A', B', and C' are conduction planes. The sodium sites are shown completely occupied. Fig. 2 (right). Schematic diagram illustrating the thermodynamic cycle of the AMTEC.

trode and the high-temperature liquid sodium exit through the wall of the device. Nearly all of the temperature drop across the AMTEC occurs in the low-pressure vapor space. A liquid return tube and an electromagnetic pump recirculate the sodium working fluid through the AMTEC to complete the cycle.

At the beginning of the AMTEC cycle, sodium at temperature T_1 from the condenser enters the hot zone and absorbs externally supplied thermal energy until it reaches T_2 . The temperature-generated pressure (chemical potential) differential across the BASE forces Na⁺ ions in the solid toward the low-pressure surface. Since BASE will conduct sodium only as Na⁺ ions, the reaction



occurs at the liquid sodium-BASE interface when sodium flows. The symbol [Na⁺]BASE indicates a sodium ion in the conduction plane of beta''-alumina. Figure 3 illustrates the molecular processes that occur across the BASE membrane and indicates the four interfaces at which sodium pressure controls the operation of the device. At open circuit, Na⁺ ions are driven by thermal kinetic energy toward the low-pressure BASE surface, causing this surface to acquire a net positive charge. The electric field in the BASE builds up until it is strong

enough to stop the flow of Na⁺. The open-circuit voltage V_{oc} is given by the Nernst equation for a concentration cell

$$V_{oc} = RT_2 F^{-1} \ln(P_2/P_4) \quad (2)$$

where R is the gas constant, F is the Faraday, P_2 is the vapor pressure of sodium at T_2 (13), and P_4 is the sodium pressure at the BASE-porous electrode interface. When the current density i across the BASE is zero, P_4 can be shown (6) to be related to the sodium vapor pressure P_1 at the condenser surface by the expression

$$P_4(i = 0) = P_1(T_2/T_1)^{1/2} \quad (3)$$

When the external circuit is closed, electrons flow through the load, neutralizing sodium ions at the BASE-porous electrode interface, reversing Eq. 1. Sodium atoms absorb their heat of vaporization, leave the porous electrode, move through the vapor space, and release their heat of condensation on the condenser surface at T_1 . The voltage developed across the BASE separator forces electrons to flow to the porous electrode through the load, producing electrical work. The initial and final states of a mole of sodium passing across the BASE from the high-pressure side to the vapor space are equivalent to an isothermal expansion from P_2 to P_4 at T_2 .

Current-Voltage Relation

A current-voltage relation for the AMTEC can be derived from Eq. 2. In this derivation we assume that the solid electrolyte is isothermal and that sodium vapor behaves as an ideal gas on the low-pressure side of the BASE. These approximations produce errors in the predicted voltage of less than 0.05 V under normal operating conditions. As current flow increases, the voltage decreases from V_{oc} because of two effects: (i) an iR_B drop occurs across the ionic resistance of the BASE, R_B , and (ii) the pressure at the electrode-BASE interface increases to drive sodium vapor through the electrode and across the vapor space.

If there is negligible resistance to sodium vapor flow in the porous electrode ($P_3 = P_4$), a simple relation can be derived between the current density, i , and the effective sodium pressure at the BASE-porous electrode interface (P_4) by using the Langmuir assumption that the rate of transport from a surface into a vacuum, n (moles per second per square centimeter), and the vapor pressure, p , of the evaporating material are linearly

related by $p = n(2\pi MRT)^{1/2}$, where M is the atomic weight. The rate of transport of sodium from interface 4 due to the electrochemical current is $n = i/F$. Thus the total effective pressure at interface 4 when current flows

$$P_4(i) = P_4(i=0) + Xi \quad (4)$$

where $X = (2\pi MRT)^{1/2}$. Substituting this expression for P_4 in Eq. 2 and subtracting the ohmic voltage drop across R_B , the resistance of the BASE, we find

$$V = A - B \ln(i + \delta) - iR_B \quad (5)$$

between the cell voltage, V , and its current density. The quantity $\delta = P_1 F(2\pi MRT_1)^{-1/2}$ represents $P_4(i=0)$, the pressure at the electrode due to evaporation of sodium from the condenser. Under normal operating conditions with $i > 0.01 \text{ A cm}^{-2}$, $T_1 < 500 \text{ K}$, and $T_2 > 800 \text{ K}$, δ can be neglected when using Eq. 5. Numerical values of the coefficients in Eq. 5 can be calculated from the thermodynamic properties of sodium (14) and the thickness and resistivity of BASE (15).

Examples of voltage versus current density calculated from Eq. 5 are shown as dashed curves in Fig. 4 for $T_2 = 983$, 1078, and 1177 K, assuming $T_1 = 500 \text{ K}$. The BASE thickness for calculating these curves was 0.08 cm. The assumptions made in the derivation of Eq. 5 are that (i) there is no pressure drop across the porous electrode, (ii) the sheet electrical resistance of the porous electrode is zero, and (iii) the BASE separator is isothermal at T_2 . These conditions have been closely approached in experimental devices. Examples of three experimental voltage-current density plots are shown as solid curves in Fig. 4 for comparison with predictions from Eq. 5. The voltages obtainable from the AMTEC are comparable to those from common galvanic cells, while the current densities are an order of magnitude larger. The high current density of the AMTEC is due to the high exchange current density present at Na-BASE interfaces (15, p. 95).

Power Density

In many applications the power density (power-to-weight ratio) is an important parameter for energy converters. The power density in an AMTEC is determined primarily by the specific power (watts per square centimeter of electrode). For an ideal electrode the specific power is given by the product Vi , V being given by Eq. 5. Since the

logarithmic term in Eq. 5 is small in comparison to the A and iR_B terms if $i > 0.1 \text{ A cm}^{-2}$, curves of specific power plotted against i are nearly parabolas, passing through $i = 0$ and $i =$ the short-

circuit current density and having a point of maximum specific power at approximately half of the short-circuit current density. The maximum specific power is a function of T_2 , T_1 , and BASE thick-

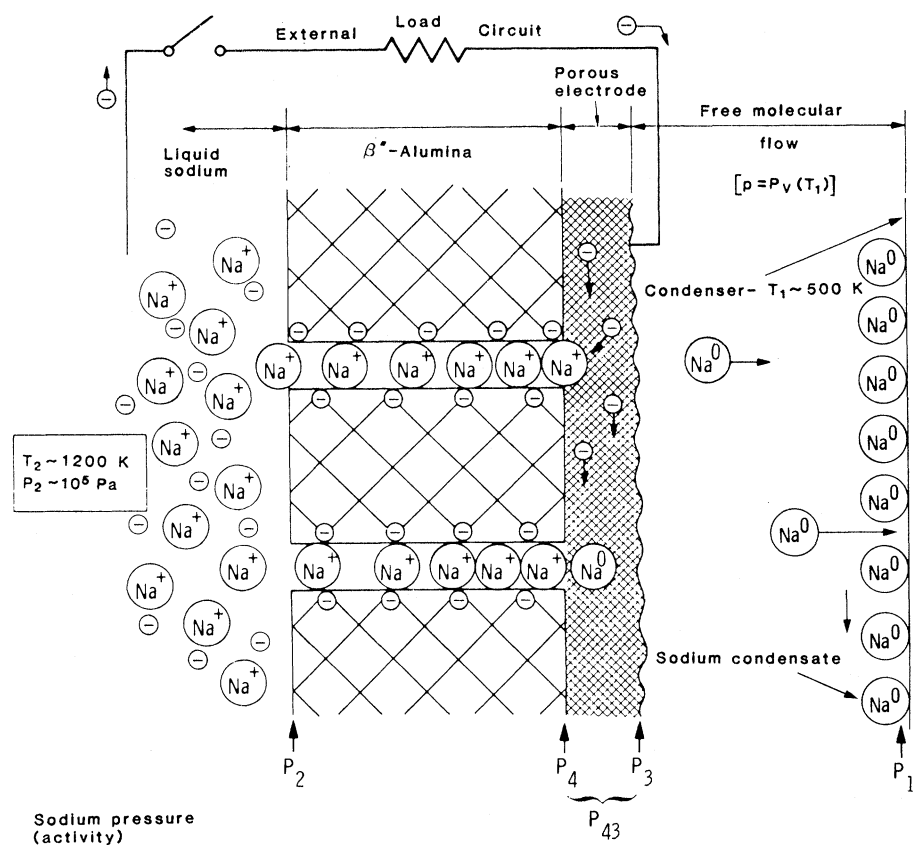


Fig. 3. Microscopic processes occurring in the solid electrolyte and at its interfaces. Although the sodium conduction planes of the BASE are shown crossing the separator without a break (single-crystal BASE), actual separators are polycrystalline sintered ceramics.

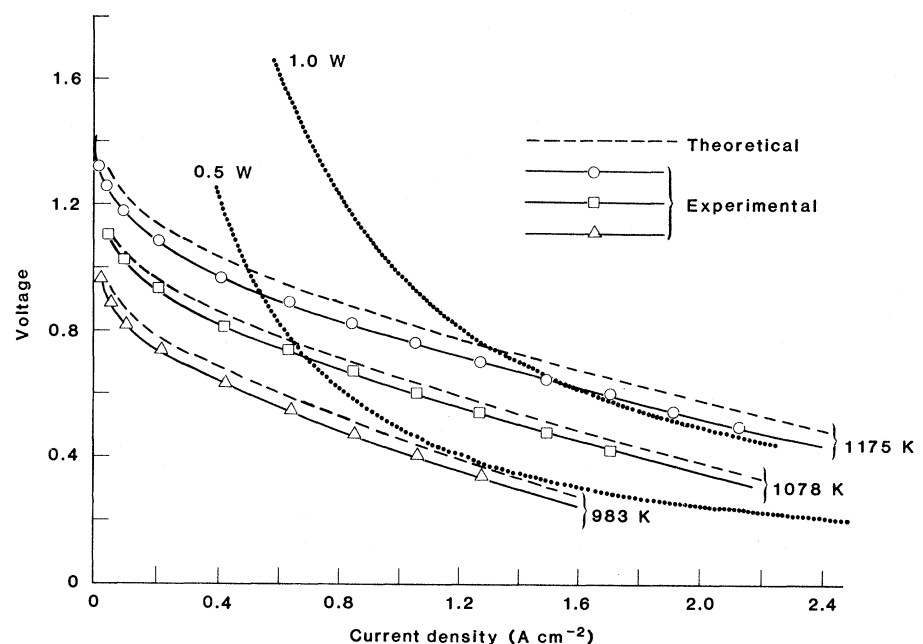


Fig. 4. AMTEC voltage-current density curves. Dashed curves are predictions of Eq. 5 with T_2 as shown and BASE 0.08 cm thick. Solid curves are experimental voltage-current density data. Dotted curves are contours of constant power in the i, V plane.

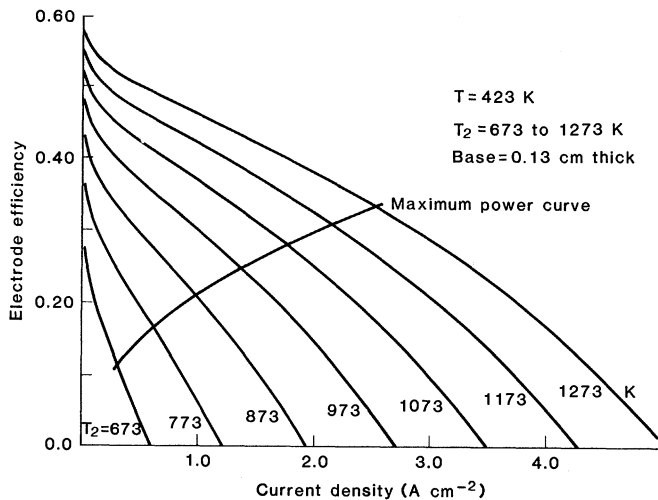


Fig. 5. Calculated curves of efficiency versus current density for an AMTEC with no conductive or radiative parasitic losses ($Q = 0$). The curve cutting through the family of efficiency curves diagonally passes through the point of maximum power for each efficiency curve.

ness. Theoretically, for a given T_1 and T_2 , maximum specific power is inversely proportional to the BASE thickness. Thus thinning the BASE could increase specific power. To date, specific powers as high as 1.1 W cm^{-2} have been achieved with BASE 0.08 cm thick; a specific power of $\sim 3 \text{ W cm}^{-2}$ appears achievable by thinning the BASE and corrugating its surface. The specific power of the AMTEC is much larger than that of conventional electrochemical power sources such as batteries and fuel cells.

Actual power densities realized in an AMTEC power system will depend on the specific design concepts; however, a rough estimate, based on a simple concentric cylindrical design can be made as follows. The mass of the BASE separator 0.12 cm thick and 1 cm^2 in area is 0.39 g ; thus, the power density of BASE alone (the mass of the porous electrode is negligible) is 3.6 kW/kg at the maximum power point for $T_2 = 1200 \text{ K}$ and $T_1 = 500 \text{ K}$. The low vapor pressure of sodium in the range 800 to 1300 K means that heavy metal walls are not required for the AMTEC. It should be possible to keep the mass of the condenser, high-temperature heat exchanger, and sodium pump to about five times the mass of the BASE, giving a power density, excluding the heat source, of 0.6 kW/kg .

Efficiency

The efficiency of the AMTEC under load is the specific output power of the electrode divided by the total heat input required per square centimeter of electrode. The input heat consists of four terms, three of which are proportional to current density:

1) The heat input to raise liquid sodium with average molar specific heat $C_p =$

30 J/K per mole from T_1 to T_2 , $iC_p(T_2 - T_1)F^{-1}$;

2) The heat to vaporize the sodium, iLF^{-1} , where the heat of vaporization $L = 89 \text{ kJ per mole}$;

3) Thermal energy equal to the electrical power output, iV ; and

4) Parasitic heat losses, Q .

In this calculation, the power required to recirculate the sodium can be neglected compared to the work output because the pump works on a virtually incompressible liquid whose molar volume is small compared to the molar volume of a gas. Thus the efficiency, η , is given by the expression

$$\eta = \frac{Vi}{i\{V + [L + C_p(T_2 - T_1)]F^{-1}\} + Q} \quad (6)$$

where Q is composed of two terms: Q_c due to heat conduction from the hot region through the output current leads and supporting structure for the BASE, and Q_r due to radiative heat loss from the porous electrode surface through the vapor space to the condenser. The Q_c term is determined by the dimensions and thermal conductivities of the electrical leads and structural members of the device, and Q_r is determined by the emissivities of the porous electrode and condenser surfaces and the geometric configuration of the device. Neither Q_c nor Q_r is prescribed by thermodynamics, and they may, in principle, be reduced to values small compared with the other terms in the denominator of Eq. 6.

By letting $Q = 0$ in Eq. 6 we obtain an expression for the maximum efficiency achievable from the AMTEC for a given T_2 , T_1 BASE thickness, and current density. We refer to this as the electrode efficiency. Figure 5 shows a family of curves for electrode efficiency versus current density over a range of T_2 with $T_1 = 500 \text{ K}$. If Q can be made smaller

than the other terms in the denominator of Eq. 6 so that the efficiency closely approaches the curves in Fig. 5, the AMTEC will be competitive with all of the well-known heat engines.

The operating efficiency of an AMTEC with porous electrode area S and two electrical leads, each having an electrical resistance R_1 and thermal conductance K_T , is

$$\eta = \frac{V - 2iSR_1}{V + V_0 + V_1 + i^{-1}(Q_r + Q_c) - iSR_1} \quad (7)$$

where

$$Q_c = K_T(T_2 - T_1)S^{-1}$$

$$Q_r = \sigma(T_2^4 - T_1^4)Z^{-1}$$

$$V_0 = LF^{-1}$$

$$V_1 = C_pF^{-1}(T_2 - T_1)$$

Here σ is the Stefan-Boltzmann radiation constant and Z is a radiation reduction factor which depends on the emissivities of the porous electrode and condenser surfaces as well as geometric view factors. Methods for calculating Z are given in textbooks on heat transfer (16).

If the porous electrode and condenser surfaces exchanged radiative energy at rates comparable to those of ideal blackbody surfaces, the maximum efficiency of the AMTEC would be less than 10 percent. However, in normal operation the condenser surface will be covered with a film of condensing liquid sodium whose reflectivity in the infrared is more than 98 percent. If the surface of the film is smooth and specular, the radiative loss can be as much as a factor of 50 below blackbody emission even if the porous electrode is an ideal emitter. To take advantage of the high specular reflectivity of the sodium condensate, the shape of the condenser surface must be designed to reflect all of the radiation emanating from the porous electrode back to the porous electrode. Laboratory working models have Z factors in the range 10 to 15, which, at $T_2 = 1200 \text{ K}$, means $Q_r \approx 1 \text{ W cm}^{-2}$. Putting a radiation shield between the porous electrode and the condenser would reduce Q_r substantially, but since the sodium vapor must traverse the same space as the radiative flux, the radiation shield would also lead to an increase in pressure at the porous electrode and thereby a reduction in cell voltage.

Figure 6 shows curves of efficiency versus specific power calculated from Eq. 7. Curve A is for a single AMTEC with $T_2 = 1200 \text{ K}$ and $T_1 = 500 \text{ K}$, $Z = 20$, and a BASE thickness of 0.1

cm. Curve B shows the effect of increasing Z to 50. The value of R_1 was optimized at each point along the curves to give the best efficiency. Each curve shows a point of maximum specific power and a point of maximum efficiency. The normal operating power range of the AMTEC would probably be selected to be in the region between these points.

Even though the efficiencies of curves A and B in Fig. 6 are impressive when compared to the 5 to 10 percent efficiencies of Seebeck effect thermoelectric generators, they can be improved still further by modifying the design to reduce the parasitic heat conduction through the electrical leads. Shrinking the cross-sectional area of the leads of a single AMTEC cell decreases the conductive heat leak Q_c but concomitantly increases the ohmic lead loss $2i^2SR_1$, since the electrical resistivity, ρ , and thermal conductivity, K_T , of metals are linked by the Wiedemann-Franz relation, $K_T\rho = \text{constant}$.

This tradeoff between thermal conductive and ohmic losses, which limits the efficiency of Seebeck effect generators, can be avoided with the AMTEC by means of a series connection of several cells, which are all at T_2 and which share a common pair of output leads. Series connection of N cells reduces the value of Q_c to Q_cN^{-1} per unit electrode area of the series-connected stack. Efficiency curve C of Fig. 6 shows the effect of connecting four cells in series and improving the Z factor to a value of 50. Curve C appears to be an attainable intermediate-term performance goal for the AMTEC. Series connection of more than four cells will not yield large efficiency gains.

Experimental Work

Experimental work on the AMTEC has been focused on two topics: (i) the structure and electrical performance of the porous electrodes and (ii) the design, construction, and testing of small working models.

Early work at Ford showed that the BASE was durable and trouble-free in the AMTEC even though the operating temperature was up to 700 K higher than that in the sodium-sulfur battery. The porous electrode, however, was found to require very careful attention. A high-performance electrode must (i) have good electrical conductivity, (ii) make a strong physical bond with low contact resistance to BASE, (iii) be highly permeable to sodium vapor, (iv) resist cor-

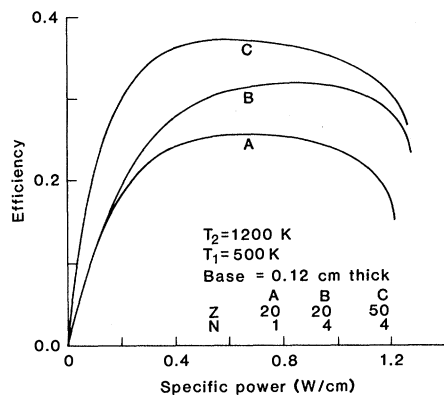


Fig. 6. Theoretical curves of operating efficiency (including parasitic losses) calculated from Eq. 8. The lead resistance R_1 was optimized at each point on the curves to give the highest efficiency. Curve A is for a single AMTEC cell with radiation reduction factor $Z = 20$. Curve B is for a single AMTEC cell with Z improved to 50. Curve C is for four cells series-connected with $Z = 50$ for each cell; it shows the efficiency improvement possible through series connection to reduce conductive thermal losses.

rosion by sodium, and (v) have a low rate of evaporation at 1300 K. These requirements are so restrictive that they rule out all but a few refractory metals and metal alloys.

Many electrodes of different composition have been deposited by a variety of techniques. To date, molybdenum and molybdenum-titanium alloy electrodes about 1 to 3 μm thick have been found to give an initial electrical performance closest to the theoretical predictions for an ideal electrode. Pure molybdenum can be deposited as a porous electrode

by chemical vapor deposition, while magnetron sputtering can produce either pure or alloy electrodes.

Electrochemical measurements on candidate electrode materials are made by depositing small patches ($\sim 1 \text{ cm}^2$) of candidate materials on a closed-end BASE tube. The tube is fitted with an internal electrical heater and the annular space between the heater and BASE filled with sodium. The electrode bearing tube is mounted inside a high-vacuum chamber after electrical leads are attached to the test electrode.

The i - V curves of freshly prepared electrodes are close to theoretical curves for ideal electrodes as shown in Fig. 4. However, all electrodes show a gradual drop in specific power output with time at high temperature. The rate of specific power loss with time increases with T_2 and varies with the porous electrode material and conditions of deposition. At a given T_2 , specific power varies in time roughly as $\exp(-at) + \text{constant}$, where a is the degradation rate constant and t the time. An asymptotic power level of 1/5 to 1/2 of the initial specific power is approached in extended tests. Transient electrochemical measurements indicate that the drop in voltage which occurs during electrode degradation is due to an increase in sodium flow resistance in the electrode. The flow resistance increase may be due to loss of pore area with sintering of the metal grains or loss of a high-permeability surface coating within the pores. By using refractory alloys such as Mo-Ti and metal- β'' -alumina composite electrodes, degradation times

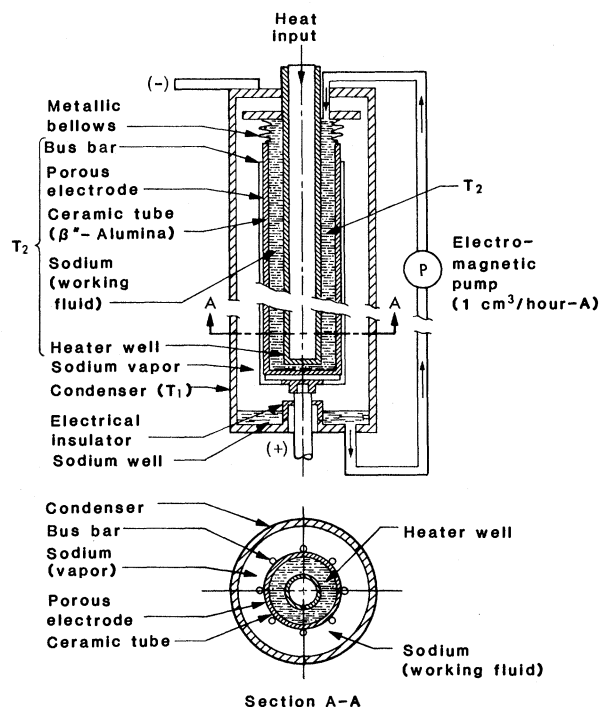


Fig. 7. Cross-sectional view of a recently tested self-contained recirculating AMTEC.

(a^{-1}) of ~ 2000 hours at a temperature of 1073 K have been achieved (17). Development of porous electrodes with a long life and high specific power is the most pressing technical issue for the AMTEC at present, and it is a current focus of AMTEC research.

Several AMTEC working models have been built and tested. Figure 7 shows a cross-sectional view of a cylindrical AMTEC cell recently tested by the Ford group (7). In this design the structure supporting the BASE tube also serves as the negative electrical lead. The device was powered by an electrical resistance heater and cooled by air convection. The BASE tube was 1.5 cm in diameter and 30 cm long, and the condenser was 6.2 cm in diameter and 50 cm long. When heated so as to simulate series-connected operation, 22 W of electrical power was produced by a thermal input of 115 W for a thermal efficiency of 19 percent (7).

Applications

An AMTEC of mature design should be an energy converter with the following characteristics: efficiency of 20 to 40 percent, power-to-weight ratio greater than 0.5 kW/kg, no moving parts, low maintenance, high durability, efficiency independent of size, modular construction, and ability to use high-temperature combustion, nuclear, or solar heat sources. Experiments to date have demonstrated the feasibility of the AMTEC and have confirmed the foregoing theoretical analysis. The cost of the AMTEC in its mature state is difficult to estimate at this early stage. There is no inherent scarcity of the materials of construction; aluminum, sodium, oxygen, ferrous alloys, and small amounts of molybdenum are plentiful. Subramanian and Hunt (18) estimate a cost of \$250 per kilowatt in batch production of a few hundred units per year. Mass production should lower this figure substantially. If improvements in durability of the porous electrode can be achieved and designs are developed to utilize some of AMTEC's unique characteristics, one can foresee a number of applications for this technology.

The AMTEC's high specific power, simplicity, potential long life, and general heat source characteristics are desirable remote power applications such as, spacecraft power sources, communication relay stations, weather buoys, military equipment, recreational vehicles, vacation homes, and construction sites.

A recent study (8) of the AMTEC as a replacement for the Si-Ge thermocouples of radioisotope thermoelectric generators, such as those now powering the Voyager spacecraft, shows that an improvement of a factor of 2 to 4 in power-to-weight ratio can be obtained with the new device.

The power output and parasitic losses in the AMTEC are proportional to the surface area of the electrode. Thus the efficiency is, to a first approximation, independent of the size of the device. By virtue of this scaling law, the AMTEC lends itself to modular construction of power-generating systems. Units of a size convenient to manufacture, say 10 to 100 kW, could be made as modules and interconnected as an array for larger power systems.

This size-independent efficiency recommends the AMTEC as a means for locally generating electrical power from chemical fuels in total energy systems (cogeneration). Widespread local generation could bring about substantial energy and capital savings relative to the present centralized system. Transmission power losses could be virtually eliminated and a few large capital investments replaced by many small ones, with capacity being added in small increments commensurate with demand growth. Furthermore, such local power generation would encourage utilization of the rejected heat from electrical generation, most of which is now wasted. On a national scale this waste heat amounts to ~ 60 percent of the energy input to electrical utilities. It is lost because low-temperature rejected heat cannot be efficiently transported from central generating plants to potential users at remote locations.

As a high-temperature topping cycle for a conventional steam power plant, the AMTEC could accept input heat at 1100 to 1300 K and produce steam at 800 K, while adding 10 to 15 percent to the plant's overall generating efficiency. As an energy converter for sodium-cooled nuclear power plants, an AMTEC energy converter would eliminate at least one heat exchanger (sodium to water) plus all high-pressure steam piping and turboalternators.

In the transportation field, the AMTEC could serve as an onboard battery charger in an AMTEC-battery hybrid electric vehicle, generating high-ampere direct current for continuous battery charging, at an efficiency comparable to a central utility, from the steady-state combustion of liquid fuel on board the vehicle. Such a vehicle could have the

range of a vehicle with a conventional internal combustion engine. The AMTEC could be adapted to burn any type of gaseous, liquid, or solid fuel. Emission control would be much easier for the ambient-pressure continuous combustion of the AMTEC than for the transient combustion of an internal combustion engine. The question of safety posed by the AMTEC's liquid sodium should be solvable because the amount of sodium would be small enough to protect or manage in an accident. It should be possible to build a 20-kW AMTEC with an inventory of less than 500 g of sodium.

Conversion of solar to electrical energy for a residential total energy system with the AMTEC at the focus of a tracking parabolic dish was recently evaluated by Subramanian and Hunt (18). They found the cost and weight per kilowatt of the AMTEC to be substantially less than those for the heat engines and electromagnetic generators now being tested for solar-to-electric conversion.

References and Notes

1. S. W. Angrist, *Direct Energy Conversion* (Allyn & Bacon, Boston, 1965).
2. H. L. Chum and R. A. Osteryoung, *Review of Thermally Regenerative Electrochemical Systems* (Report TR-332-416 Solar Energy Research Institute, Golden, Colo., 1981).
3. J. T. Kummer and N. Weber, U.S. patent 3,458,356 (1968).
4. N. Weber, *Energy Convers.* **14**, 1 (1974).
5. T. K. Hunt, N. Weber, T. Cole, *Proc. 10th Intersoc. Energy Convers. Eng. Conf.* (1975), part 2, p. 231.
6. ———, *Proc. 13th Intersoc. Energy Convers. Eng. Conf.* (1978), p. 2011.
7. ———, in *Fast Ionic Transport in Solids*, J. B. Bates and G. C. Farrington, Eds. (North-Holland, New York, 1981), p. 263.
8. C. P. Bankston, T. Cole, R. Jones, R. Ewell, *AIAA J.* (July–August 1983).
9. T. Cole, in *Proceedings of a Workshop on Thermally Regenerative Electrochemical Systems*, H. L. Chum, Ed. (Report CP-234-1577, Solar Energy Research Institute, Golden, Colo., 1981).
10. J. B. Bates, J.-C. Wang, N. J. Dudney [*Phys. Today* **35** (No. 7), 46 (1982)] give a list of background references on solid electrolytes.
11. J. B. Bates and G. C. Farrington, Eds., *Fast Ionic Transport in Solids* (North-Holland, New York, 1981).
12. Ceramtec Inc., Salt Lake City, Utah.
13. The chemical potential of sodium at T_2 is given more precisely by the expression $RT_2 \ln(P_2) + P_h V_m$, where P_2 is the vapor pressure at T_2 , P_h is the hydrostatic pump pressure in excess of P_2 , and V_m is the molar volume of the liquid sodium. This second term is negligible in comparison to the logarithmic term.
14. H. G. Bommelberg and C. R. F. Smith, in *Sodium-NaK Engineering Handbook*, O. J. Foust, Ed. (Gordon & Breach, New York, 1972), vol. 1, pp. 1–168.
15. T. K. Hunt, N. Weber, T. Cole, in *Proceedings of an International Conference on Fast Ion Conduction in Solids*, P. Vashishta, J. N. Mundy, G. K. Shenoy, Eds. (North-Holland, New York, 1979), p. 277.
16. R. Siegel and J. R. Howell, *Thermal Radiation Heat Transfer* (McGraw-Hill, New York, 1972).
17. N. Weber, private communication.
18. K. Subramanian and T. K. Hunt, *Proc. 17th Intersoc. Energy Convers. Eng. Conf.* (1982), p. 1474.
19. The research described in this article was carried out in part by Jet Propulsion Laboratory, California Institute of Technology, under contract with the National Aeronautics and Space Administration.